Nanotechnology **19** (2008) 335203 (6pp) doi:10.1088/0957-4484/19/33/335203

Tuning shades of white light with multi-color quantum-dot–quantum-well emitters based on onion-like CdSe–ZnS heteronanocrystals

Hilmi Volkan Demir[1], Sedat Nizamoglu[1], Evren Mutlugun[1], Tuncay Ozel[1], Sameer Sampra[2], Nikolai Gaponik[2] and Alexander Eychmüller[2]

[1] Department of Physics, Department of Electrical and Electronics Engineering, Nanotechnology Research Center, and Institute of Materials Science and Nanotechnology, Bilkent University, Ankara 06800, Turkey
[2] Physical Chemistry, TU Dresden, Bergstraße 66b, D-01062 Dresden, Germany

E-mail: volkan@bilkent.edu.tr

Received 4 March 2008, in final form 5 June 2008
Published 7 July 2008
Online at stacks.iop.org/Nano/19/335203

Abstract
We present white light generation controlled and tuned by multi-color quantum-dot–quantum-well emitters made of onion-like CdSe/ZnS/CdSe core/shell/shell heteronanocrystals integrated on InGaN/GaN light-emitting diodes (LEDs). We demonstrate hybrid white LEDs with (x, y) tristimulus coordinates tuned from (0.26, 0.33) to (0.37, 0.36) and correlated color temperatures from 27 413 to 4192 K by controlling the number of their integrated red–green-emitting heteronanocrystals. We investigate the modification of in-film emission from these multi-layered heteronanocrystals with respect to their in-solution emission, which plays a significant role in hybrid LED applications. Our proof-of-principle experiments indicate that these complex heteronanocrystals hold promise for use as nanoluminophors in future hybrid white LEDs.

(Some figures in this article are in colour only in the electronic version)

As an alternative to conventional means of lighting, solid state lighting offers energy saving, reliability and safety [1]. Because of these favorable benefits, white light-emitting diodes (WLEDs) are in great demand. To date different types of WLEDs (e.g. multi-chip WLEDs, monolithic WLEDs and color-conversion WLEDs) have been investigated [2–4]. Among them, color-conversion WLEDs have been the most widely used and those based on phosphor coatings have been commercially available since 1996 [5]. In such WLEDs, typically a blue LED excites yellow YAG phosphors and the resulting blue electroluminescence from the LED and yellowish photoluminescence from the phosphors together generate white light. However, although phosphors conveniently provide broadband photoemission for color conversion, there are problems associated with their usage. Some of these problems include low color rendering index due to dual-color mixing and changes in the optical properties of the generated white light with input power [6]. Also, the broad emission spectrum of phosphors makes it relatively difficult to fully tune the emission spectrum of the generated white light. Due to these disadvantages, novel luminescent materials are under investigation [7].

Among various luminescent materials, semiconductor quantum-dot nanocrystals (NCs) have attracted a great deal of attention because of their size-tunable photoluminescence, high photoluminescence quantum yields and high photostability. The use of NCs has been explored for a wide range of applications including photodetectors, photovoltaics, lasers and sensors [8–14]. Among different applications, white light-emitting devices draw significant attention because of their

potential widescale use and large market. To date color-conversion WLEDs that integrate combinations of CdSe/ZnS core–shell nanocrystals on blue InGaN/GaN LEDs have been successfully demonstrated [15]. Such hybrid NC-WLEDs that provide warm-white light with high color rendering index have also been realized [16]. Moreover, WLEDs based on the integration of both fluorescent polymers and nanocrystals have also been shown [17, 18]. A WLED that consists of a blue/green two-wavelength InGaN/GaN LED integrated with red NCs has been reported [19]. Furthermore, a white LED has also been fabricated on a commercial UV-LED coated with a mixture of CdSeS NCs [20] and by using layer-by-layer assembly of CdSe/ZnS NCs on a near-UV LED [21, 22]. However, all of these hybrid NC-WLEDs rely on the use of mono-color-emitting nanocrystals or their multiple combinations as luminophors.

Only recently multi-color-emitting semiconductor heteronanocrystals (hetero-NCs) have been demonstrated by Battaglia *et al* using a quantum-dot–quantum-well (QDQW) structure in the CdSe–ZnS material system [23]. In this nested structure, first a CdSe core, then a ZnS barrier shell, and finally a CdSe well shell are synthesized one after the other, outer layers surrounding inner ones. By using these multi-layered CdSe–ZnS hetero-NCs in solution, white light generation with multi-color emission from their CdSe cores (in yellow–orange) and from their CdSe shells (in cyan) has been accomplished [24]. However, these orange–cyan-emitting heteronanocrystals in solution are not sufficient for white light generation on a LED platform in the solid state. For that reason, emission properties of these heteronanocrystals need to be carefully analyzed [25] and they need to be implemented in the solid form for proper integration on a LED platform to generate white light [26]. In this paper, unlike the previous work of ours and others, we present white light generation precisely controlled and tuned by multi-color-emitting quantum-dot–quantum-well heteronanocrystals integrated on InGaN/GaN light-emitting diodes for the first time. In this study, tuning photometric properties of white light with such multi-color emitters enables application-specific lighting with optimal spectral content, e.g. for street lighting at night and museum display lighting indoors.

Our multi-color light emitters, made of onion-like CdSe/ZnS/CdSe core/shell/shell heterostructures, are designed and synthesized to emit in red (around 600 nm) from the CdSe core and in green (around 550 nm) from the CdSe shell. By careful design and hybridization of these multi-layered red–green-emitting heteronanocrystals on blue-emitting LEDs, we demonstrate hybrid integrated WLEDs on a single chip. These hybrid hetero-NC-WLEDs are implemented in a well-controlled manner with their (x, y) tristimulus coordinates tuned from (0.26, 0.33) to (0.37, 0.36) across the CIE chromaticity diagram as shown in figure 1, along with their corresponding correlated color temperatures tuned from 27 413 to 4192 K and the luminous efficacy of their optical radiation (i.e. the ratio of their emitted luminous flux to their radiant flux) tuned from 258 to 375 lm W^{-1} (in lumens per watt of optical power). The tuning of these photometric properties is conveniently controlled by the

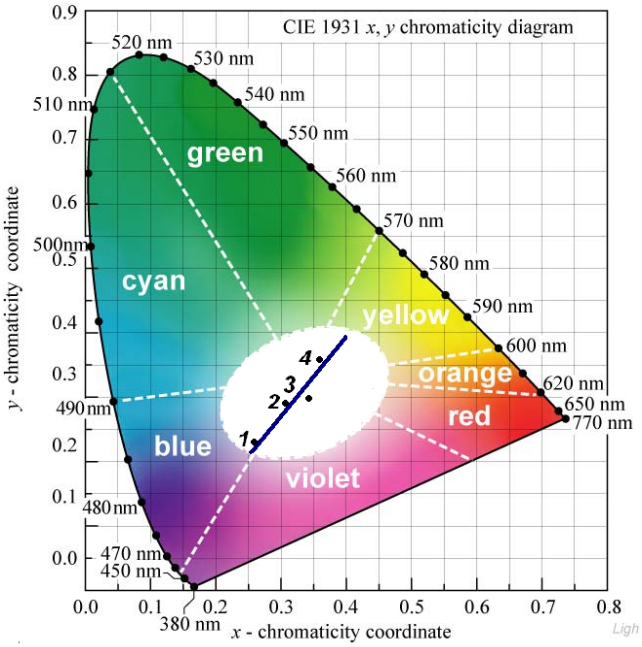

Figure 1. Tuning shades of white light with multi-color quantum-dot–quantum-well emitters made of onion-like CdSe/ZnS/CdSe core/shell/shell heteronanocrystals integrated on InGaN/GaN light-emitting diodes (hetero-NC-WLEDs 1–4) across the CIE (1931) chromaticity diagram.

number of integrated heteronanocrystals. Related to tuning, we investigate the modification of in-film emission from these multi-layered heteronanocrystals with respect to their in-solution emission. This plays a significant role in the use of these complex heteronanocrystals in hybrid LED applications.

These hybrid hetero-NC-WLEDs operate on the principle that the integrating LED base optically excites the integrated heteronanocrystal film as the nanoluminophors. For that, when electrically driven in forward bias, the LED emits in the blue to optically pump the integrated heteronanocrystals that in turn luminesce in red and in green. Consequently, the multi-color photoluminescence of these hetero-NCs and the single-color electroluminescence of the LED together generate white light, if designed properly. To use as the luminophor layer, we synthesize multi-layered CdSe/ZnS/CdSe core/shell/shell heteronanocrystals [24]. Their synthesis starts with making CdSe core NCs [27]. For that, 0.1 mmol CdO is dissolved in 0.83 mmol OA and 4 ml ODE and heated at 300 °C under Ar atmosphere. Another solution of Se/TOP/ODE (0.05 mmol/0.5 ml/0.5 ml) is dissolved at 100 °C. The Se/TOP/ODE solution is then injected into the colorless Cd/OA/ODE solution at 300 °C. The temperature is reduced to 280 °C and heating is continued for 30 s at this temperature. The nanocrystals are separated by precipitation and redissolved in hexane. 10^{-7} mol of these NCs, 3 g hexadecylamine (HDA) and 3 ml ODE are added and heated to 200 °C. Subsequently, a colorless solution (0.1 M) of ZnO and OA (1:4 ratio) in 10 ml ODE is prepared by heating the mixture to 300 °C. The Cd/OA, S and Se/TBP solutions, all 0.1 M, are used for overcoating to make shells. Adequate amounts of the Zn (Cd) and S (Se) solutions required for one shell growth are added to the core

Table 1. Photoluminescence peak wavelengths of the synthesized onion-like CdSe/ZnS/CdSe heteronanocrystals in solution and in film (samples 1–4).

	Peak wavelengths (nm)	
Samples	Shell emission peak	Core emission peak
Reference (in solution)	558.42	613.32
Sample 1 (in film)	561.75	602.17
Sample 2 (2 × hetero-NCs in sample 1)	562.74	604.64
Sample 3 (4 × hetero-NCs in sample 1)	560.48	612.62
Sample 4 (9 × hetero-NCs in sample 1)	569.44	621.53

Table 2. Photoluminescence relative peak intensities of the synthesized onion-like CdSe/ZnS/CdSe heteronanocrystals in solution and in film (samples 1–4).

	Relative intensity (au)	
Samples	Shell emission peak	Core emission peak
Reference (in solution)	0.695	0.156
Sample 1 (in film)	0.573	0.152
Sample 2 (2 × hetero-NCs in sample 1)	0.609	0.145
Sample 3 (4 × hetero-NCs in sample 1)	0.228	0.668
Sample 4 (9 × hetero-NCs in sample 1)	0.136	0.820

CdSe NCs and the heating is continued for 30 min. Small aliquots of the reaction mixture are recovered, precipitated with acetone and finally dissolved in toluene.

For blue InGaN/GaN light-emitting diodes, we use a GaN dedicated metal–organic chemical vapor deposition (MOCVD) system (Aixtron RF200/4 RF-S) [28, 29]. We first grow a 14 nm thick GaN nucleation layer and a 200 nm thick GaN buffer layer. Then follows a 690 nm thick, Si-doped n-type contact layer. Subsequently, we continue the epitaxial growth with five 4–5 nm thick InGaN/GaN quantum structures as the active layers of our LEDs. We use an active region growth temperature of 661 °C to obtain an electroluminescence peak around 450 nm. Finally, we finish our growth with p-type layers that contain Mg-doped, 50 nm thick $Al_{0.1}Ga_{0.9}N$ and 120 nm thick GaN layers as the contact cap. Following the growth, we activate Mg dopants at 750 °C for 15 min. To construct device mesas and electrical contacts, we use photolithography, thermal metal evaporation, reactive ion etch and rapid thermal annealing, among the standard semiconductor processing procedures also performed in our previous work [30–33]. The p-contacts consist of Ni/Au (15 nm/100 nm) annealed at 700 °C for 30 s under N_2 and the n-contacts consist of Ti/Al (100 nm/2500 nm) annealed at 600 °C for 60 s under N_2. For integration of the hetero-NCs on the LEDs with a cross-sectional active area of 300 μm × 300 μm, we make relatively uniform closely packed heteronanocrystal films on them, controlling their film thickness with the right starting amount of their corresponding NC solutions. After taking the necessary amount from the heteronanocrystal–toluene solution, we add acetone and centrifuge the resulting mixture to precipitate the hetero-NCs. We then disperse the heteronanocrystals in chloroform solvent and drop-cast them on the LED in controlled amounts. By post-baking over 10 min, we completely evaporate the solvent for proper hetero-NC film formation. Such InGaN–GaN-based LEDs are demonstrated to achieve long lifetimes, around tens of thousands of hours [34], and CdSe–ZnS-based nanocrystal emitters are stated to exhibit shelf lifetimes of thousands of hours [35].

A variety of physical mechanisms including reabsorption, dipole–dipole interaction, energy transfer and effective dielectric constant change of the environment significantly alter optical emission properties of the nanocrystals, typically leading to a redshift in their luminescence when cast in solid film with respect to their luminescence when in solution. To investigate these luminescence modifications of the heteronanocrystals in films compared to in solution and its significance in device implementation of WLEDs, we synthesize CdSe/ZnS/CdSe heteronanocrystals with emission originating from the CdSe core and CdSe shell. The in-solution luminescence that comes from the CdSe core has its peak at 613 nm and the one from the shell at 558 nm. The long-wavelength emission from the core is confirmed by only red emission after the synthesis of the core. For investigating in-film luminescence redshift with respect to in-solution luminescence, we prepare four samples of heteronanocrystal films with different heteronanocrystal amounts precisely in integer multiples (1, 2, 4 and 9 multiples) of the starting sample (ca. 1 nmol). Tables 1 and 2 show the photoluminescence (PL) peak wavelengths and relative peak intensities of these samples (samples 1–4) excited with an He–Cd laser at 325 nm at room temperature. As the number of heteronanocrystals in each sample increases, we observe that all emission peaks experience redshifts in the film and that the relative intensities of emission at shorter wavelengths decrease (due to the reabsorption, dipole–dipole interaction, energy transfer, etc). However, with respect to the in-solution PL (reference), the peak (with emission at 613 nm in solution) generated by the CdSe core in the thin films (samples 1–4) experiences a blueshift as shown in table 1. Here this significant blueshift is attributed to the effect of the substrate, which decreases with increasing number of nanocrystals [36]. Excitons localized both in the CdSe core and the CdSe shell of a hetero-NC are indeed expected to be affected by the substrate. However, since the excitons in the shells of different nanocrystals in the film state are closer to each other, the dipole interaction between the nanocrystals is considered to be more dominant for the shells, effectively leading to a redshift in the shell emission despite the substrate effect. Moreover, for samples 1–4, it is interesting to note that, although the peak coming from the CdSe core experiences a redshift of 8.2 nm going from sample 1 to sample 4, the peak (with emission 558 nm in solution) coming from the CdSe shells experience a redshift of 11.0 nm. As a result, the shells exhibit a larger redshift in comparison to the core in the thin films. We consider the additional redshift compared to the core is due to the collectivization of the electronic states as our hetero-NCs do not have any outermost ZnS potential barrier that can prevent the occurrence

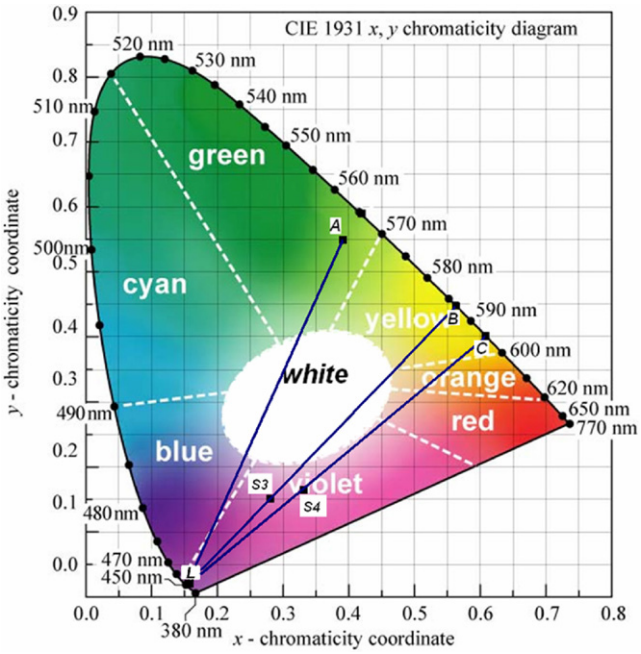

Figure 2. The tristimulus coordinates of electroluminescence from the blue LED (L), the tristimulus coordinates of photoluminescence from the heteronanocrystals in solution (A), the tristimulus coordinates of the total emission from the integrated hybrid hetero-NC-LEDs (S3 and S4), and the effective tristimulus coordinates of the photoluminescence only contributed from the heteronanocrystals integrated on the blue LED for S3 and S4 (B and C, respectively), for the investigation of the resulting redshift (from A to B to C) across the CIE (1931) chromaticity coordinates.

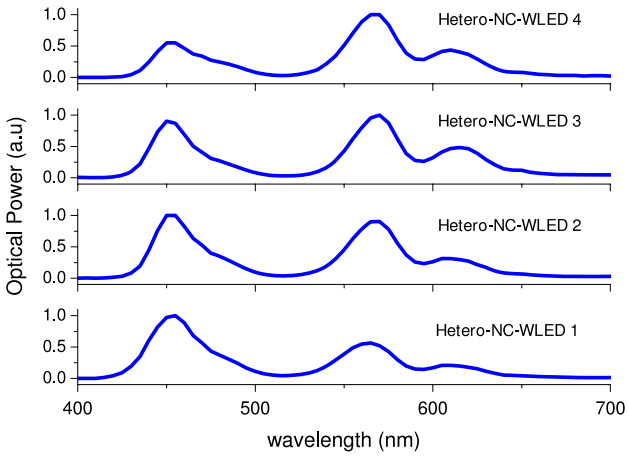

Figure 3. Emission spectra of our hybrid white light-emitting diodes (hetero-NC-WLEDs 1–4).

of the coupled states. At this point, it is also worth discussing that, although these onion-like heteronanocrystals have been previously [23] and also in our work [24, 26] shown to exhibit multi-color emission in solutions and in films, a further study on the single-nanocrystal level needs to be conducted to verify the multiple nature of this emission. However, these present discussions will still remain valid regardless of whether the single heteronanocrystals exhibit multiple color emission or not.

To further analyze the effect of the redshift in the solid form in device implementation we hybridize hetero-NCs with the same amounts of samples 3–4 on the blue LED and investigate the resulting shift of the effective (x, y) tristimulus coordinates across the CIE chromaticity diagram. In figure 2, the point L represents the operating point of the starting blue LED at (0.14, 0.03), while the points S3 and S4 at (0.27, 0.10) and (0.33, 0.12) represent the coordinates of the hybrid WLEDs integrated with the heteronanocrystals (with the amounts of samples 3 and 4) integrated on the blue LED, respectively. On the other hand, the point A at (0.39, 0.55) indicates the in-solution luminescence of the heteronanocrystals, while the point B at (0.52, 0.45) and the point C at (0.61, 0.40) show the effective (x, y) tristimulus coordinates of the collective luminescence contributed only from the integrated heteronanocrystals (excluding the LED contribution itself) on the hybrid devices of S3 and S4, respectively. Here we determine the effective tristimulus coordinates (B and C) by extrapolating a line from the blue LED operating point at (0.14, 0.03) through the hybrid device operating points (S3 and S4, respectively); the resulting end points of these extrapolated lines crossing the boundary on the chromaticity diagram give the effective tristimulus points to represent the effective color contribution solely from the hetero-NCs in the film on these hybrid platforms. The conventional boundary of the chromaticity coordinate is drawn by transforming each mono-color in the visible represented as a Dirac function using the color matching functions. Since we define these effective tristimulus coordinates on the boundary of the chromaticity diagram, they represent their effective contributing colors, each being mathematically equivalent to a specific Dirac function on the chromaticity diagram. When we look at the shift of these coordinates from A to B to C, we clearly observe the effect of the heteronanocrystals' in-film redshift with respect to their in-solution luminescence on the chromaticity diagram. This redshift makes it harder to obtain white light generation in films in general. In figure 2, the line that connects the operating points of the blue LED and the in-solution PL of hetero-NCs passes through the white region, implying that white light generation was possible with these hetero-NCs should there be no redshift in the film. However, in figure 2, the in-film redshift makes it impossible to obtain white light generation for the hybrid device implementations with these heteronanocrystals in the film because the line segments L − S3 and L − S4 do not intersect the white region. This redshift in the luminescence of the solid heteronanocrystals is inevitable and should be carefully taken into account to obtain white light using solid heteronanocrystals on an LED platform.

To obtain white light generation, by considering the luminescence redshift in film with respect to in solution, we synthesize heteronanocrystals with the core emission at 602 nm and the shell emission at 550 nm. For sample hetero-NC-WLED 1, we hybridize 0.33 nmol heteronanocrystals on the blue LED. We obtain the white light emission spectrum shown in figure 3 with the tristimulus coordinates of (0.26, 0.23) falling in the white region of the CIE choromaticity diagram, as shown in figure 1, along with a color temperature of

Table 3. Photometric characteristics of our hybrid white hetero-NC-WLEDs (1–4).

Hetero-NC-WLED	Number of nanocrystals (nmol)	X	Y	Correlated color temperature (K)	Optical luminous efficacy (lm W^{-1})
1	0.33	0.26	0.23	27 413	258
2	0.40	0.31	0.29	6 780	313
3	0.46	0.34	0.30	4 635	315
4	0.50	0.37	0.36	4 192	375

27 413 K and a luminous efficacy of the emitted spectrum of 258 lm W^{-1}. From hetero-NC-WLEDs 1–4, we gradually increase the number of hybridized heteronanocrystals on the blue LED as shown in table 3. As a result, the color temperature decreases because the relative contribution coming from the heteronanocrystals with respect to the blue LED emission increases. Finally, for hetero-NC-WLED 4, we integrate 0.50 nmol heteronanocrystals to generate white light with a warmer color temperature. The operating point corresponds to the tristimulus coordinates of (0.50, 0.37) in the white region, the correlated color temperature decreases to 4192 K and the luminous efficacy of the emitted spectrum reaches a relatively high value of 375 lm W^{-1}. As a result, from hetero-NC-WLEDs 1–4 we tune the optical properties of the generated white light with varying (x, y) tristimulus coordinates from (0.26, 0.33) to (0.37, 0.36), correlated color temperature from 27 413 to 4192 K and luminous efficacy of the emitted spectra from 258 to 375 lm W^{-1} by precisely controlling the number of integrated heteronanocrystals.

In conclusion, we presented white light generation controlled and tuned by hybridization of CdSe/ZnS/CdSe core/shell/shell multi-color-emitting heteronanocrystals on blue-emitting InGaN/GaN LEDs. We showed white hybrid hetero-NC-LEDs with varying (x, y) tristimulus coordinates from (0.26, 0.33) to (0.37, 0.36), correlated color temperatures from 27 413 to 4192 K, and luminous efficacies of optical radiation from 258 to 375 lm W^{-1} by controlling the number of integrated heteronanocrystals. Furthermore, we discussed that the redshift in-film emission of the heteronanocrystals with respect to the in-solution emission has a significant effect on hybrid WLED implementation and has to be carefully taken into account for the proper design of such hybrid hetero-NC-WLEDs.

Acknowledgments

This work is supported by EU-PHOREMOST Network of Excellence 511616 and Marie Curie European Reintegration Grant MOON 021391 and by TUBITAK under project nos. 106E020, 107E088, 107E297, 104E114, 105E065 and 105E066. Also, HVD acknowledges additional support from the Turkish Academy of Sciences Distinguished Young Scientist Award (TUBA GEBIP) and the European Science Foundation (ESF) European Young Investigator Award (EURYI) Programs. The authors are also pleased to acknowledge using the facilities of the Bilkent University Nanotechnology Research Center (founder Professor E Ozbay) and Advanced Research Laboratories and Institute of Materials Science and Nanotechnology (founder Professor S Ciraci).

References

[1] Hirosaki N, Xie R, Kimoto K, Sekiguchi T, Yamamoto Y, Suehiro T and Mitomo M 2001 *Appl. Phys. Lett.* **79** 211905
[2] Schubert E F 2006 *Light-Emitting Diodes* (Cambridge: Cambridge University Press)
[3] Yamada M, Narukawa Y, Tamaki H, Murazaki Y and Mukai T 2005 *IEICE Trans. Electron* **E88-C9** 1860
[4] Chen H, Yeh D, Lu C, Huang C, Shiao W, Huang J, Yang C C, Liu I and Su W 2006 *IEEE Photon. Technol. Lett.* **18** 1430
[5] Nakamura S and Fasol G 1997 *The Blue Laser Diode* (Berlin: Springer)
[6] Kim J S, Jeon P E, Park Y H, Choi J C, Park H L, Kim G C and Kim T W 2004 *Appl. Phys. Lett.* **85** 3696–8
[7] Nag A and Sarma D D 2007 *Chem. Mater.* **111** 13641
[8] Qi D, Fischbein M B, Drndic M and Selmic S 2005 *Appl. Phys. Lett.* **86** 093103
[9] Gur I, Fromer N A, Geier M L and Alivisatos A P 2005 *Science* **310** 462–5
[10] Mutlugun E, Soganci I M and Demir H V 2007 *Opt. Express* **15** 1128–34
[11] Klimov V, Mihkailovsky A, Xu S, Malko A, Hollingsworth J, Leatherdale C and Bawendi M 2000 *Science* **290** 314–7
[12] Mutlugun E, Soganci I M and Demir H V 2008 *Opt. Express* **16** 3537–45
[13] Somers R C, Bawendi M G and Nocera D G 2007 *Chem. Soc. Rev.* **36** 579–91
[14] Soganci I M, Nizamoglu S, Mutlugun E, Akin O and Demir H V 2007 *Opt. Express* **15** 14289–98
[15] Nizamoglu S, Ozel T, Sari E and Demir H V 2007 *Nanotechnology* **18** 065709
[16] Nizamoglu S, Zengin G and Demir H V 2008 *Appl. Phys. Lett.* **92** 031102
[17] Demir H V, Nizamoglu S, Ozel T, Mutlugun E, Huyal I O, Sari E, Holder E and Tian N 2007 *New J. Phys.* **9** 362
[18] Ahn J H, Bertoni C, Dunn S, Wang C, Talapin D V, Gaponik N, Eychmüller A, Hua Y, Bryce M R and Petty M C 2007 *Nanotechnology* **18** 335202
[19] Chen H, Yeh D, Lu C, Huang C, Shiao W, Huang J, Yang C C, Liu I and Su W 2006 *IEEE Photon. Technol. Lett.* **18** 1430
[20] Ali M, Chattopadhyay S, Nag A, Kumar A, Sapra S, Chakraborty S and Sarma D D 2007 *Nanotechnology* **18** 075401
[21] Nizamoglu S and Demir H V 2007 *J. Opt. A: Pure Appl. Opt.* **9** S419
[22] Nizamoglu S and Demir H V 2007 *Nanotechnology* **18** 405702
[23] Battaglia D, Blackman B and Peng X 2005 *J. Am. Chem. Soc.* **127** 10889
[24] Sapra S, Mayilo S, Klar T A, Rogach A L and Feldmann J 2007 *Adv. Mater.* **19** 569
[25] Nizamoglu S and Demir H V 2008 *Opt. Express* **16** 3515–26
[26] Nizamoglu S, Mutlugun E, Ozel T, Demir H V, Sapra S, Gaponik N and Eychmüller A 2008 *Appl. Phys. Lett.* **92** 1131110
[27] Qu L, Peng Z A and Peng X G 2001 *Nano Lett.* **1** 333
[28] Sari E, Nizamoglu S, Ozel T and Demir H V 2007 *Appl. Phys. Lett.* **90** 011101

[29] Ozel T, Sari E, Nizamoglu S and Demir H V 2007 *J. Appl. Phys.* **102** 113101
[30] Demir H V, Sabnis V A, Fidaner O, Harris J S Jr, Miller D A B and Zheng J F 2005 *IEEE J. Sel. Top. Quantum Electron.* **11** 86
[31] Demir H V, Sabnis V A, Fidaner O, Harris J S Jr, Miller D A B and Zheng J F 2004 *Opt. Express* **12** 310
[32] Sabnis V A, Demir H V, Fidaner O, Harris J S, Miller D A B, Zheng J F, Li N, Wu T C, Chen H T and Houng Y M 2004 *Appl. Phys. Lett.* **84** 469
[33] Demir H V, Sabnis V A, Zheng J F, Fidaner O, Harris J S and Miller D A B 2004 *IEEE Photon. Technol. Lett.* **16** 2305
[34] Tsao J Y 2004 *IEEE Circuits Devices Mag.* **20** 3
[35] Evident Technologies 2007 http://www.evidenttech.com/products/evidots/evidot-specifications.html?searched_shelf_lifetime&_ajaxSearch_highlight_ajaxSearch_highlight1_ajaxSearch_highlight2_
[36] Chistyakov A A, Martynov I L, Mochalov K E, Oleinikov V A, Sizova S V, Ustinovich E A and Zakharchenko K V 2006 *Laser Phys.* **16** 1625